Influence of reconstruction on the surface state of Au(110)

Andreas Nuber,[1,*] Mitsuharu Higashiguchi,[2] Frank Forster,[1] Peter Blaha,[3] Kenya Shimada,[4] and Friedrich Reinert[1,5]
[1]*Experimentelle Physik II, Universität Würzburg, Am Hubland, D-97074 Würzburg, Germany*
[2]*Graduate School of Science, Hiroshima University, Higashi-Hiroshima 739-8526, Japan*
[3]*Institute of Materials Chemistry, Vienna University of Technology, Getreidemarkt 9/165, A-1060 Vienna, Austria*
[4]*Hiroshima Synchrotron Radiation Center, Hiroshima University, Higashi-Hiroshima 739-0046, Japan*
[5]*Forschungszentrum Karlsruhe, Gemeinschaftslabor für Nanoanalytik, D-76021 Karlsruhe, Germany*
(Received 21 August 2008; revised manuscript received 17 October 2008; published 12 November 2008)

We present high-resolution angle-resolved photoelectron spectroscopy on Au(110). The unreconstructed surface shows a Shockley-type surface state at E_0=590 meV whereas on the (2×1) missing-row reconstructed surface no such surface state below E_F can be detected. We performed relativistic local-density approximation calculations which agree well with our experimental data. Adsorption of 1 monolayer Ag on the (2×1) reconstructed surface results in a destruction to a (1×1) surface structure and a Shockley state appears at E_0=475 meV. Shifting down the surface state from just above to below E_F by Na adsorption allowed to extrapolate a binding energy on the reconstructed surface of E_0=−120 meV above the Fermi level.

DOI: 10.1103/PhysRevB.78.195412 PACS number(s): 73.20.At, 68.35.B−, 79.60.Bm

I. INTRODUCTION

Shockley surface states on metal systems were investigated for several years since they are among the most important two-dimensional model systems. They appear in the gaps of projected bulk states and can be observed on various metal surfaces, such as the (111) faces of noble metals (Cu, Ag, Au) which were thoroughly investigated.[1–3] Shockley states are confined to the topmost atomic layers and hence form a two-dimensional electronic system. The in-plane dispersion $E_B(k_\parallel)$ of the Shockley states can be approximated by a parabola representing a nearly free-electron behavior. Investigations on the meV scale can give insights into many-body interactions such as electron-electron and electron-phonon interactions resulting in a deviation from the parabolic dispersion and energy-dependent linewidth broadening.[3–5] Due to their localization on the surface, Shockley states are very sensitive to surface modifications such as adsorbates and surface reconstructions.[3,6–11] For example, 1 monolayer (ML) deposition of Ag on a Cu(111) surface leads to two different (9×9) surface reconstructions; as a consequence the Shockley surface states have unequal maximum binding energies of E_0=310 meV for the moiré structure and E_0=241 meV for the triangular structure.[12]

The (110) faces of Cu, Ag, and Au are expected to show Shockley states having the same origin and similar properties as the ones on the (111) faces. For Cu(110) and Ag(110) this has been verified[13,14] but there are some inconsistent reports in literature about the occupied Shockley-type surface state on the Au(110) surface.[15–17] Heimann *et al.*[15] and Courths *et al.*[16] reported about the observation of a surface state at the $\bar{Y}$ point of the surface Brillouin zone (SBZ) with a binding energy of $E_0\approx-0.1$ eV, whereas, Sastry *et al.*[17] did not observe any surface state at $\bar{Y}$ on the Au(110) surface.

The obvious difference between Au(110) and the other noble metals is an interesting issue. It is well known that Au(111) reconstructs in the herringbone structure having an influence on the Shockley state[3] whereas Cu(111) and Ag(111) appear unreconstructed as well as their (110) faces.[13,14,18,19] This paper focuses on the Au(110) surface,[15,16] the surface reconstruction,[17,20,21] and its influence on the Shockley state.

Additionally we used Na and Ag as adsorbates to manipulate the surface state. As shown on the systems Na/Au(111) (Ref. 9) and Na/Cu(111) (Ref. 6) submonolayers of alkali atoms shift the Shockley state continuously down due to electron donation and a work-function change. In contrast, monolayers of Ag result in a discrete shift of the surface state in direction of the binding energy of the clean Ag(111) surface which has been demonstrated for Ag/Au(111) and Ag/Cu(111).[7,10] Furthermore, the Shockley state of Au(111) shows a *k*-dependent spin-orbit splitting derived from the breakdown of inversion symmetry at the surface.[2] A similar splitting may be expected at the Shockley state of Au(110). We used high-resolution angle-resolved photoelectron spectroscopy (ARPES) in the vacuum ultraviolet (VUV) range to study the electronic structure just below the Fermi level (E_F) and low-energy electron diffraction (LEED) to determine the surface structure of Au(110).

The Au(110) surface is known to reconstruct at room temperature to the (2×1) missing-row structure.[17,20,21] Figure 1 shows a schematic diagram of the three-dimensional (3D) Brillouin zone of a fcc lattice and the construction of the rectangular SBZ of the (110) face (left panel). The (2×1) missing-row reconstruction halves the short aspect of the SZB ($\overline{\Gamma Y}$ direction) therefore the $\bar{Y}$ point of the unreconstructed SBZ becomes the new $\bar{\Gamma}'$ point of the (2×1) reconstructed SBZ. The SBZ of the unreconstructed and the reconstructed Au(110) with all relevant high-symmetry points are shown in the right panel in Fig. 1. The high-symmetry points of the (2×1) reconstructed surface are indicated by a prime.

II. EXPERIMENTAL DETAILS

The measurements have been performed at the undulator beamline (BL-1) at the synchrotron (HiSOR) in Hiroshima (Japan) using a Scienta SES 200 analyzer and *p*-polarized light with photon energies $h\nu$=40–60 eV (Ref. 22) and at

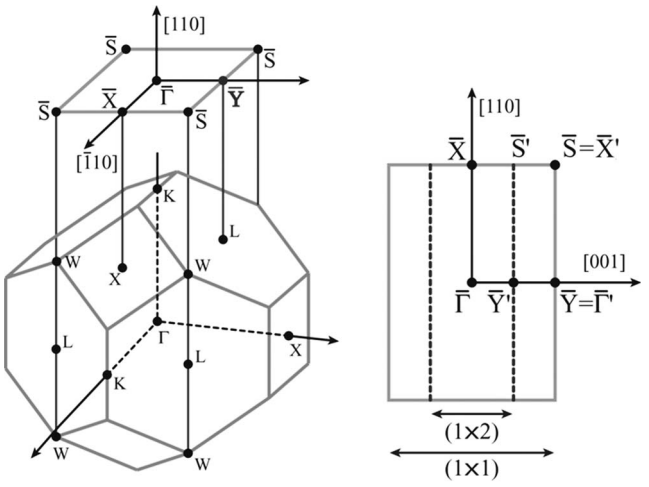

FIG. 1. Construction of the (110) face two-dimensional SBZ from the 3D Brillouin zone of a fcc lattice (left). SBZ of unreconstructed (1×1) as well as (2×1) missing-row reconstructed Au(110) (right).

the laboratory in Würzburg, with a Scienta R4000 analyzer and a monochromated He discharge lamp (Gammadata VUV 5010). In the laboratory we used He I_α ($h\nu$=21.2 eV) and He II_α ($h\nu$=40.8 eV). The sample was measured and cooled on liquid-He-flow-type manipulators with five and four degrees of freedom, respectively (measuring temperature was $<$20 K). The base pressure of the spectrometer chambers was lower than 2×10^{-10} mbar but using the VUV lamp the pressure rose up to 1.3×10^{-9} mbar due to He leakage. The preparation chambers contained an electron bombardment heating setup, sputter guns, LEED optics, and diverse metal evaporation sources. The angle resolution was $\Delta\Theta=0.3°$ ($\approx$0.01 Å^{-1} for He I_α) and the energy resolution was $\Delta E \approx 10$ meV for the ARPES measurements. The ARPES measuring direction was along $\overline{YS}$ of the unreconstructed SBZ and $\overline{\Gamma' X'}$ of the reconstructed SBZ (former $\overline{YS}$ of the unreconstructed SBZ). $\bar{Y}$ and $\overline{\Gamma'}$ are located at k_x=0.77 Å^{-1} with respect to $\bar{\Gamma}$ (normal emission).

For the preparation of unreconstructed Au(110) we used a new mechanically polished crystal from Mateck GmbH, Germany and treated it with mild sputter-annealing cycles using a low-intensity Ar^+ ion beam with an energy of 1–2 keV and a subsequent annealing at 400 °C.[22] The sample preparation for the (2×1) reconstructed Au(110) consisted of repeated thorough sputter-annealing cycles using a high-intensity Ar^+ ion beam (about 50$\times$ higher ion flux) with an energy of 1.5 keV and subsequent annealing to 500 °C for 20 min. The cleanliness has been checked by Auger electron spectroscopy (AES), x-ray photoelectron spectroscopy (XPS), and ultraviolet photoelectron spectroscopy (UPS). The surface structure was checked by Fermi-surface mapping and LEED.

For the deposition of Ag we used a resistively heated effusion cell stabilized at a temperature of T=1200 °C resulting in a deposition rate of approximately 0.3 ML/min. The sample was cooled down to $T\approx200$ K before Ag deposition. To get smooth, well-ordered films the sample was warmed after Ag deposition up to room temperature for about 10 min. For Na deposition the sample was kept at T=70 K during the exposure under the Na dispenser (SAES-Getters) for several seconds. The Na dispenser was operated at a deposition rate of about 0.01 ML/s (estimated by XPS experiments).

III. CLEAN AU(110)

The ARPES measurements on clean unreconstructed Au(110), measured with $h\nu$=50 eV, show the parabolic-shaped Shockley state dispersion in a hardly visible gap as displayed in Fig. 2(a). The photoemission intensity is given on a grayscale versus binding energy E_B and parallel momentum k_y. The k_y axis of the momentum parallel to the surface was chosen to point along the $\overline{YS}$ direction. The sample was also orientated to measure along $\overline{YS}$. With the assumption of a nearly free-electron behavior, the Shockley state parameters have been obtained by a parabolic fit to the ARPES data. The maximum binding energy E_0 was found to be 590 ± 5 meV at the $\bar{Y}$ point. The band mass $m^*=(0.25\pm0.01)m_e$ in $\overline{YS}$ direction. Since the surface state on Au(110) does not exhibit a cylindrical symmetry like the one on Au(111), the band mass is maximal along the $\overline{YS}$ direction while it is minimal along the $\overline{Y\Gamma}$ direction.[23]

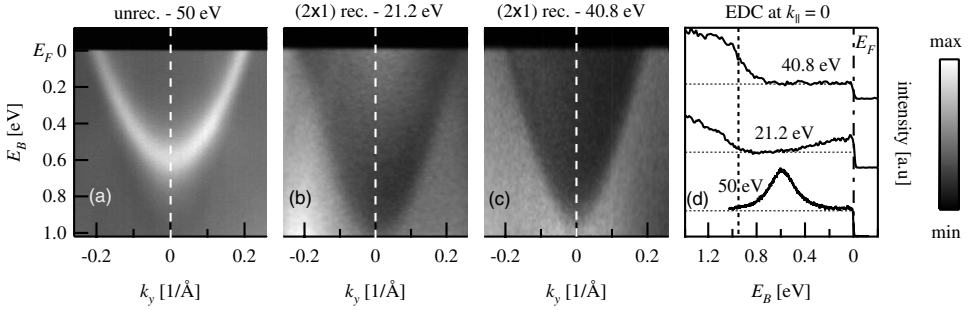

FIG. 2. Photoemission data on clean Au(110). The photoemission intensity $I(E_B,k_y)$ is given on a grayscale (high intensities appear bright) versus binding energy E_B and parallel momentum k_y measured along $\bar{S}\leftarrow\bar{Y}\rightarrow\bar{S}$ (unrec.) and $\overline{X'}\leftarrow\overline{\Gamma'}\rightarrow\overline{X'}$ (rec.). (a) The photoemission data were taken on an unreconstructed surface with $h\nu$=50 eV. It shows a parabola-shaped surface state in a hardly visible gap; (b) was measured on a (2×1) reconstructed surface with He I_α ($h\nu$=21.2 eV); a distinct gap without any surface state can be seen. (c) shows the same with He II_α excitation ($h\nu$=40.8 eV). (d) shows the EDCs at k_y=0 ($\overline{\Gamma'}$ or $\bar{Y}$) marked by the dashed lines in (a)–(c). E_F is indicated by the dash-dotted line, the bulk gap edge by the dashed line, and the background by the horizontal dotted lines.

The two-dimensional character of the observed Shockley state was verified by ARPES measurements with different excitation energies ($h\nu$=[40–60] eV, data not shown) in which the surface state did not show any changes in energy and therefore has no dispersion in $k_\perp$.

The sample preparation as described above resulted in a well-ordered (2×1) missing-row reconstructed Au(110) surface. ARPES spectra measured with the He I_α and He II_α excitation lines, displayed in Figs. 2(b) and 2(c), respectively, show no surface state at $\bar{\Gamma}'$ below E_F but a distinct empty Au bulk band gap. The two upper energy distribution curves (EDCs) at $\bar{Y}'=\bar{\Gamma}'$ (k_y=0 Å^{-1}, k_x=0.77 Å^{-1}) displayed in Fig. 2(d) show the empty gap at $\bar{\Gamma}'$ with the gap edge at a binding energy of approximately 1 eV. Due to the (2×1) reconstruction the former $\bar{Y}$ point becomes the new $\bar{\Gamma}'$ point and hence the electronic states from $\bar{Y}$ should be backfolded to the $\bar{\Gamma}$ point at normal emission and vice versa. In fact ARPES measurements on the (2×1) reconstructed Au(110) surface show the observed gap also at normal emission which is not seen on a nonreconstructed surface.

The lowest curve in Fig. 2(d) gives an EDC at $\bar{Y}$ which shows the Shockley state of clean unreconstructed Au(110). Its full width at half maximum (FWHM) of approximately 250 meV is quite high which could be due to a nonperfect surface[24] with many step edges and defects judging from the relatively high background intensity within the band gap. However these defects may stabilize the unreconstructed surface over large areas of the sample surface. We should also note that the clean unreconstructed Au(110) surface prepared by the same conditions is highly reproducible, giving the same Fermi surface and band dispersions of the Shockley states. Calculated surface energies of the unreconstructed as well as (2×1) reconstructed Au(110) surfaces are summarized in Ref. 25 and references therein. The differences between unreconstructed and (2×1) reconstructed Au(110) surfaces range from −0.58 to −5 meV/Å^2.

Figure 3 shows Fermi-surface maps (FSMs) of (a) calculated unreconstructed Au(110), (b) photoemission data of unreconstructed Au(110) ($h\nu$=50 eV), and (c) photoemission data of (2×1) reconstructed Au(110) ($h\nu$=21.1 eV). The photoemission intensity at E_F is displayed on a grayscale versus the components of momentum k_x and k_y parallel to the surface. High-symmetry points are indicated by crossing solid lines and labeled between the panels. The FSMs of unreconstructed Au(110) [(a) and (b) in Fig. 3] cover one full SBZ in $\bar{\Gamma}\bar{Y}$ direction. The Shockley states are visible as bright ellipses around $\bar{Y}$ with the semimajor axis in $\bar{Y}\bar{S}$ direction (maximum band mass). Due to polarization effects, the outer parts of the ellipses appear dark. Around the $\bar{\Gamma}$ point no features are visible neither a distinct electronic state nor band gap. Hence the periodicity of the FSM of the full (unreconstructed) SBZ is an evidence for an unreconstructed Au(110) surface, whereas the lower panel (c) of Fig. 3 in contrast shows the FSM of the (2×1) reconstructed surface with the doubled periodicity in $\bar{\Gamma}\bar{Y}$ direction with respect to the unreconstructed SBZ. Here, clearly the gaps at all three visible $\bar{\Gamma}'$ points can be seen. The bright features crossing the FSM in the lower panel are *sp*-type bulk bands. They are backfolded due to the surface reconstruction but these backfolded bands exhibit a low intensity since their wave functions have only small weight at the surface where the reconstruction takes place.

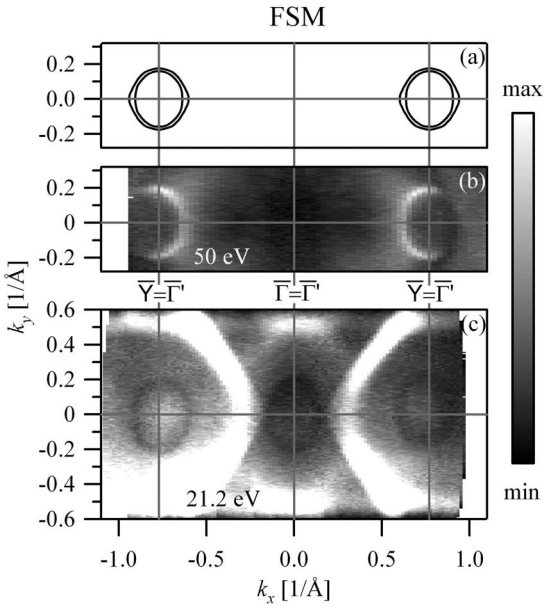

FIG. 3. Fermi-surface maps of (a) calculated unreconstructed Au(110), (b) photoemission data of unreconstructed Au(110) ($h\nu$ =50 eV), and (c) photoemission data of (2×1) reconstructed Au(110) ($h\nu$=21.1 eV). High intensities appear bright and high-symmetry directions are marked by lines. The doubled periodicity of the SBZ for the (2×1) reconstructed surface is clearly visible in $\bar{\Gamma}\bar{Y}$ direction.

The Shockley state on Au(111) shows a *k*-dependent spin-orbit (SO) splitting due to the loss of inversion symmetry at the surface. The Au(111) surface can be prepared with large terraces and only few defects resulting in a small FWHM of 27 meV at $\bar{\Gamma}$ making the SO splitting detectable by ARPES.[4] One can anticipate that a similar splitting might be observable on the Shockley state of unreconstructed Au(110). However, we could not resolve such a splitting since the FWHM of 250 meV, determined from the EDC at $\bar{Y}$, is too large in this case. Earlier calculations[26,27] did not consider any spin-orbit splitting.

IV. THEORY

In order to check whether the SO interaction of the Shockley state of Au(110) could be detected with our experimental resolution and whether it is comparable to the SO interaction of the surface state of Au(111), we performed a relativistic first-principles self-consistent LDA slab-layer calculation utilizing the WIEN2K code for the unreconstructed and the (2×1) missing-row reconstructed Au(110) surfaces. The used slabs consist of 21 Au layers surrounded by a vacuum region of 19 Å. The spin-orbit splitting of the surface states can be estimated by comparison of relativistic (including SO) and scalar relativistic (without SO) calculations since there is always an artificial splitting due to the

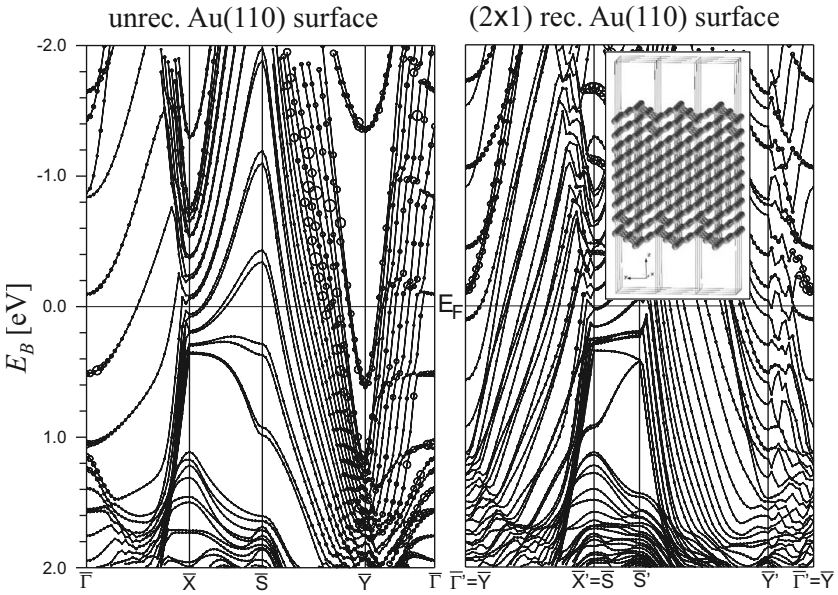

FIG. 4. LDA slab-layer calculation of an unreconstructed (left panel) and (2×1) reconstructed (right panel) Au(110) surface. Inset shows the used slab for the (2×1) reconstructed surface. The diameter of the circles indicates the surface character of the electronic states.

spurious interaction of the two surfaces of the finite slab cell. The calculations have been performed along the high-symmetry directions of the unreconstructed and (2×1) reconstructed surfaces. Figure 4 shows the calculated band structure of unreconstructed (left panel) and (2×1) reconstructed (right panel) Au(110). The diameter of the circles indicates the magnitudes of the surface character of the electronic states. At the $\bar{Y}$ point of the unreconstructed surface there is a band below E_F with a high surface character and well separated from other states, with a maximum binding energy of $E_0=(607\pm5)$ meV. The indicated error was derived from the finite slab related uncertainties. This is in agreement with calculations from Liu *et al.*[26] who also predict a surface state close to and below the Fermi level on an ideal unreconstructed Au(110) surface. We calculated the FSM of this spin-orbit split surface related band on unreconstructed Au(110) shown in Fig. 3(a) which is in agreement with our photoemission data (b). The bulge in $\overline{\Gamma Y}$ direction is an artifact from the finite slab size. The spin-orbit splitting in $\overline{YS}$ direction with $\Delta k=(0.005\pm0.001)$ Å^{-1} is small in comparison to $\Delta k=(0.024\pm0.001)$ Å^{-1} for the Shockley state of Au(111).[8] The evaluated splitting is corrected for the artificial splitting from the finite slab size. Since the k resolution of the used setup for He I_α is $\Delta k\approx0.01$ Å^{-1} the calculated splitting in $\overline{YS}$ direction is not resolvable in our measurements.

Due to the bisection of the SBZ in $\overline{\Gamma Y}$ direction on a (2×1) missing-row reconstructed surface the former $\bar{Y}$ point becomes a new $\overline{\Gamma'}$ point and backfolding of the electronic states occurs. Hence the surface state now is located at $\overline{\Gamma'}$. Since the reconstruction is very massive, the surface state shifts $\approx$700 meV to lower binding energies over the Fermi level to a binding energy of $E_0=(-118\pm5)$ meV. Also other bands with some weight at the surface shift in energy and change dispersion. We should note here that the parabolic energy bands below E_F for (2×1) reconstructed Au(110) are mainly derived from the bulk. These bands merge to a weak continuous background in the limit of infinite thickness of the slab which can be neglected for the present discussion of the surface-state dispersion. Xu *et al.*[27] obtained by calculation a surface state just above E_F on a (2×1) reconstructed Au(110) surface in agreement with our results but without considering spin-orbit interaction. However, our calculations result in a spin-orbit splitting of the surface state of $\Delta k=(0.012\pm0.001)$ Å^{-1} that would be resolvable with our experimental setup. But the surface state is completely above E_F and hence not accessible by ARPES.

In Fig. 5 the calculated bands are plotted over measured ARPES data in $\bar{S}\leftarrow\bar{Y}\rightarrow\bar{S}$ and $\overline{X'}\leftarrow\overline{\Gamma'}\rightarrow\overline{X'}$ direction, respectively. The binding energy of the surface state (S) at $\bar{Y}$ on the unreconstructed surface is reproduced very well ($E_0^{\mathrm{LDA}}=(607\pm5)$ meV, $E_0^{\mathrm{exp}}=(590\pm5)$ meV) but also the dispersion ($m^*_{\mathrm{LDA}}=(0.16\pm0.02)m_e$, $m^*_{\mathrm{exp}}=(0.25\pm0.01)m_e$) and the band gap are in agreement. The spin-orbit splitting is clearly visible as two shifted parabolas. The splitting is not corrected for finite slab effects and hence overestimated. This can obviously be seen by the finite splitting at the $\bar{Y}$ point since spin-orbit split bands should be degenerate at high-symmetry points as a consequence of the combination of time reversal and translational symmetry. Additionally, the data for (2×1) reconstructed Au(110) are well reproduced in

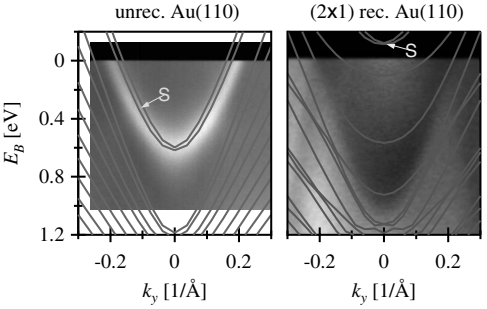

FIG. 5. LDA calculations plotted over photoemission data of unreconstructed (left panel, $\bar{S}\leftarrow\bar{Y}\rightarrow\bar{S}$) and (2×1) reconstructed (right panel, $\overline{X'}\leftarrow\overline{\Gamma'}\rightarrow\overline{X'}$) Au(110). The split surface states (s) are marked; all other shown bands originate from the bulk. The splitting contains SO plus spurious interaction (see text).

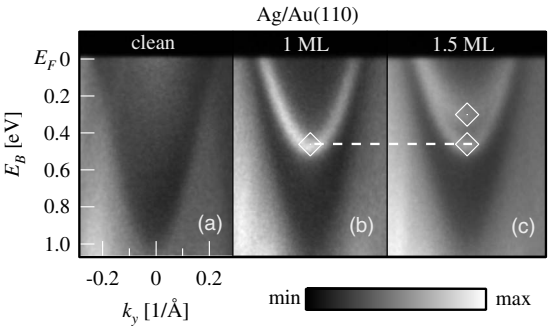

FIG. 6. Photoemission data of (a) clean Au(110), (b) 1 ML, and (c) 1.5 ML Ag on Au(110). The diamonds indicate the maximum binding energy E_0 of the surface state at $\bar{\Gamma}'$.

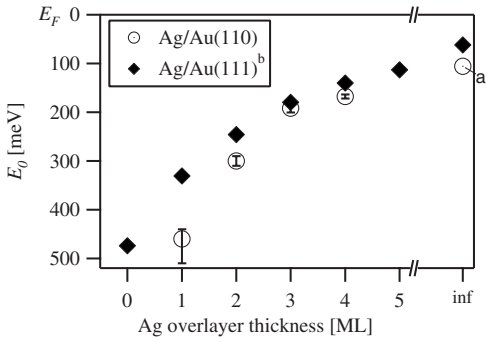

FIG. 7. Comparison of the surface-state maximum binding energies E_0 of Ag-monolayer coverages on Au(111) and Au (110), respectively. Diamonds represent Ag/Au(111) and circles Ag/Au(110). The two systems show a similar behavior [(a) from Ref. 14 and (b) from Ref. 7)].

that there are no distinct surface-derived states below E_F around the $\bar{\Gamma}$ point. It should be noted that the spin-orbit split surface state (S in Fig. 5) appears closely above E_F.

V. MODIFICATION BY ADSORBATES

Since surface states are localized at the surface they are very sensitive to adsorbates and the surface structure.[3,6–11,28,29] In order to get a better understanding of the Shockley state on Au(110) we adsorbed Ag and Na on the surface. Ag deposition on Au(111) leads to an ordered layer-by-layer growth. The surface state shows a discrete shift from the binding energy of a clean Au(111) crystal to the binding energy on a clean Ag(111) crystal.[10] With each additional Ag layer, the surface state becomes more Ag-like since the wave function of the surface state decays exponentially into the bulk within a few monolayers.[29] The system Ag/Au(110) shows an analogous behavior: Fig. 6 contains photoemission data at $\bar{Y}$ of an initially (2×1) reconstructed Au(110) with different Ag coverages. Spectrum (a) shows clean (2×1) reconstructed Au(110) with its empty gap for comparison. A surface state emerges after 1 ML Ag is adsorbed with a binding energy of $E_0=(475\pm5)$ meV, displayed in spectrum (b). After deposition of additional 0.5 ML, a second surface state emerges at a lower binding energy $[E_0=(300\pm5)$ meV], shown in (c), which can be attributed to the areas of the sample surface with 2 ML Ag coverage. A comparison between the binding energies of the Shockley states of the systems Ag/Au(111) ($\bar{\Gamma}$ point) and Ag/Au(110) ($\bar{Y}$ point) is shown in Fig. 7. The evolution of the Shockley state binding energies with Ag coverage is similar from the clean Au (left) to the clean Ag values (right) whereas the value for clean Au(110) is missing since there is no Shockley state below E_F on the reconstructed surface. LEED data show that the adsorbed Ag layers destruct the (2×1) missing-row reconstruction of Au(110) to a (1×1) pattern. Figures 8(a) and 8(b) show representative LEED images for clean (2×1) reconstructed Au(110) and 1 ML Ag/Au(110). For the clean reconstructed surface the LEED data show a (2×1) pattern with respect to the bulk terminated (110) face of the fcc lattice consisting of sharp spots with low background which indicates a well-ordered surface. On Ag adsorption the LEED spots related to the reconstruction disappear leaving a (1×1) pattern. This suggests that after the surface destruction coming along with 1 ML Ag deposition the Shockley state evolves with further adsorption as on unreconstructed Au(110) and hence is located below E_F.

We additionally could destroy the (2×1) reconstructed Au(110) surface by adsorption of 0.5 ML (Ref. 30) of Au on the cold ($T=15$ K) sample. We obtained a (1×1) LEED pattern and observed the evolution of a surface state in the bulk band gap by ARPES (data not shown) which is an additional evidence for the influence of the surface structure on the energetic position of the Shockley state on Au(110).

More insights into the issue where the Shockley state is situated or if it exists at all on reconstructed Au(110) were obtained by Na deposition. Our and former calculations,[27] as well as experimental data from inverse photoemission,[31] suggest a surface state above E_F on the (2×1) reconstructed surface. Earlier, submonolayer Na deposition was successfully used to shift the Shockley state of noble metals down to higher binding energies.[6,9] This suggests to use this method for shifting down the Shockley state of (2×1) reconstructed Au(110) from just above E_F to binding energies below E_F in order to make it accessible by ARPES. Figure 9 shows a series of ARPES measurements on (2×1) reconstructed Au(110) with increasing Na coverage in the submonolayer range (0–0.4 ML). The unaltered projected bulk band gap is clearly visible in all spectra whereas a parabolic surface state continuously shifts below E_F with increasing Na coverage. By linear extrapolation to a clean surface, indicated by the dashed line of the maximum binding energies, a binding energy of $E_0=(-120\pm30)$ meV was estimated for the Shock-

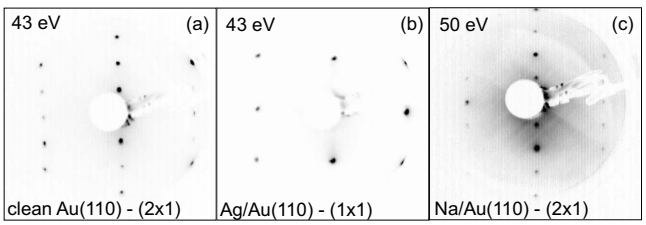

FIG. 8. LEED images of a clean (2×1) reconstructed Au(110) surface, (1×1) unreconstructed 1 ML Ag/Au(110), and (2×1) reconstructed Na/Au(110).

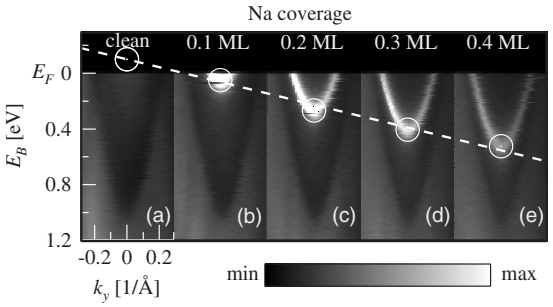

FIG. 9. Photoemission data of (2×1) rec. Au(110) with different coverages of Na. The clean (2×1) rec. Au(110) surface shows an empty gap at $\overline{\Gamma'}$. Exposure to Na leading to a submonolayer coverage shifts down the surface state. Circles indicate the maximum binding energies of the surface states and the dashed line represents the linear extrapolation to a clean surface.

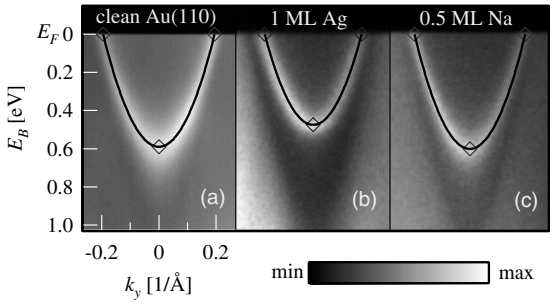

FIG. 10. Comparison between clean unreconstructed Au(110), 1 ML Ag/Au(110), and 0.5 ML Na/Au(110). Dark lines indicate a parabolic fit to the data (k_F and E_0).

ley state of clean (2×1) Au(110). LEED measurements show that Na adsorption on the reconstructed surface does not change the LEED pattern [see Fig. 8(c)] except for an increase in the background intensity and spot width and a decrease in spot intensity which can be explained by the increasing disorder due to the statistically distributed Na atoms. Hence, the Na adsorption in the low-coverage regime does not alter the surface structure and therefore the continuous surface-state shift is not induced by surface structural change but only by a decreased work function and electron transfer as described above. This legitimates the extrapolation from the Na adsorption series to a clean reconstructed surface, as demonstrated in Fig. 9. Lindgren and Walldén[6] explained the increase in binding energy of the Shockley state on the system Na/Cu(111) by the large work-function change $\Delta\phi$ on Na deposition. The continuous decrease in the low-coverage regime of up to $\Delta\phi\approx2.7$ eV depending on the amount of Na is related to a strong polarization of the adsorbed Na atoms. This leads to a decreasing potential in the surface region which explains the observed surface-state shift[6,32] and suggests a charge transfer of Na $3s$ electrons into the former unoccupied surface state.[9]

A comparison between the measured occupied surface states with comparable binding energies of clean unreconstructed Au(110), 1 ML Ag/Au(110), and 0.5 ML Na/Au(110) are displayed in Fig. 10. Parabolic fits are indicated by solid lines. Points of maximum binding energy E_0 and intersection points of the surface states and the Fermi energy are marked by diamonds. The observed linewidths, obtained from EDCs at $\overline{Y}$ or $\overline{\Gamma'}$, are a measure for the surface quality in terms of defect density and terrace widths. Adsorbed Na atoms act as defects, therefore the FWHM increases linearly with Na coverage from 100 to 200 meV for coverages of 0.2–0.8 ML. Ag adsorption results in well ordered films resulting in FWHMs of ≈60 meV. In contrast the surface state on the unreconstructed Au(110) surface shows a large FWHM of 250 meV due to defects and step edges which in turn stabilize the unreconstructed surface as described above. Typical values for the linewidth of other (110) surfaces states amount to 48 meV for unreconstructed Cu(110) and ≤50 meV for Ag(110).[33,34] Table I summarizes parameters

TABLE I. Summary of Shockley state parameters obtained from ARPES measurements and DFT slab-layer calculations. Negative values for the binding energy E_0 indicate a location above E_F. Since m^* of the surface state on Au(110) exhibits different values in different directions m^*, k_F, and Δk for Au(110) have been evaluated in $\overline{YS}$ or $\overline{\Gamma'X'}$ direction, respectively, in which they are maximal.

	E_0 (meV)	m^*/m_e [a]	k_F (Å^{-1}) [a]	Δk (Å^{-1}) [a]
Au(111)[b]	481 ± 2	0.260 ± 0.005	$0.169/0.193\pm0.001$	0.024
LDA Au(111)[c]	484	0.22		0.031
Au(110) unrec.	590 ± 5	0.25 ± 0.01	0.195 ± 0.005	
LDA Au(110) unrec.	607 ± 5	0.16 ± 0.02	$0.166/0.171\pm0.001$ [e]	0.005 ± 0.001 [e]
Au(110) (2×1) rec.[d]	-120 ± 30	0.24 ± 0.02		
LDA Au(110) (2×1) rec.	-118 ± 5	0.23 ± 0.02		0.012 ± 0.001 [e]
1 ML Ag/Au(110)	475 ± 5	0.23 ± 0.01	0.169 ± 0.005	
≈0.5 ML Na/Au(110)	601 ± 5	0.22 ± 0.01	0.188 ± 0.005	

[a]For Au(110) evaluated in YS or $\Gamma'X'$ direction, respectively.
[b]From Ref. 9.
[c]From Ref. 8.
[d]Values extrapolated from Na/Au(110).
[e]Corrected for artificial slab related splitting.

for the dispersion of the Shockley state obtained from our investigation both calculated by LDA and measured by ARPES for the (110) faces along with published values for Au(111).

VI. CONCLUSION

We studied the Shockley state of unreconstructed and (2×1) reconstructed Au(110) clean surfaces by means of low-temperature high-resolution ARPES. We also used different adsorbates to manipulate the surface state and compared the results to analogous systems on Au(111). On clean unreconstructed Au(110) our ARPES measurements show a surface state with a maximum binding energy of $E_0=(590\pm5)$ meV whereas on (2×1) reconstructed Au(110) no surface state below E_F could be detected. No spin-orbit splitting of the Shockley state could be resolved. We performed relativistic LDA calculations which are in agreement with our experimental findings and show a shift of the surface state due to the reconstruction of about 700 meV across E_F. Adsorbing Ag on the (2×1) reconstructed Au(110) surface resulted in the destruction of the surface to a (1×1) surface structure and hence to an appearance of a Shockley state at $E_0=(475\pm5)$ meV. The behavior of the surface states on further Ag deposition is analogous to the system Ag/Au(111). By Na adsorption we were able to shift the Shockley state continuously from just above to clearly below E_F. A linear extrapolation gives a binding energy of $E_0=(-120\pm30)$ meV above E_F for the clean (2×1) reconstructed Au(110) surface and hence a surface-state shift of more than 700 meV due to the surface reconstruction. Even without any chemical modification the surface state on Au(110) shows this tremendous change in energy of the order of 1 eV only due to surface reconstruction. Our results give a comprehensive understanding of the Shockley state on Au(110) surfaces and the influence of surface reconstruction and selected adsorbates on it. Due to the found sensitiveness of the Shockley state on sample preparation and impurities the inconsistencies in literature could be attributed to sample preparation and characterization.

ACKNOWLEDGMENTS

M.H. and F.R. thank the Japan Society for the Promotion of Science for financial support. The synchrotron-radiation experiments were done under the approval of HSRC (Proposal No. 06-A-50). This work was supported generously by the Deutsche Forschungsgemeinschaft (Grant No. RE1469/4-4) and the BMBF (Grant No. 05KS7WW1).

*Corresponding author; andreas.nuber@physik.uni-wuerzburg.de

[1] S. D. Kevan and R. H. Gaylord, Phys. Rev. B **36**, 5809 (1987).
[2] S. LaShell, B. A. McDougall, and E. Jensen, Phys. Rev. Lett. **77**, 3419 (1996).
[3] F. Reinert and G. Nicolay, Appl. Phys. A: Mater. Sci. Process. **78**, 817 (2004).
[4] F. Reinert, G. Nicolay, S. Schmidt, D. Ehm, and S. Hüfner, Phys. Rev. B **63**, 115415 (2001).
[5] A. Eiguren, B. Hellsing, F. Reinert, G. Nicolay, E. V. Chulkov, V. M. Silkin, S. Hüfner, and P. M. Echenique, Phys. Rev. Lett. **88**, 066805 (2002).
[6] S. A. Lindgren and L. Walldén, Solid State Commun. **34**, 671 (1980).
[7] L. Huang, X. G. Gong, E. Gergert, F. Forster, A. Bendounan, F. Reinert, and Z. Y. Zhang, Europhys. Lett. **78**, 57003 (2007).
[8] F. Forster, A. Bendounan, F. Reinert, V. G. Grigoryan, and M. Springborg, Surf. Sci. **601**, 5595 (2007).
[9] F. Forster, A. Bendounan, J. Ziroff, and F. Reinert, Surf. Sci. **600**, 3870 (2006).
[10] H. Cercellier, Y. Fagot-Revurat, B. Kierren, F. Reinert, D. Popovic, and D. Malterre, Phys. Rev. B **70**, 193412 (2004).
[11] A. Bendounan, F. Forster, J. Ziroff, F. Schmitt, and F. Reinert, Phys. Rev. B **72**, 075407 (2005).
[12] A. Bendounan, F. Forster, J. Ziroff, F. Schmitt, and F. Reinert, Surf. Sci. **600**, 3865 (2006).
[13] P. Heimann, J. Hermanson, H. Miosga, and H. Neddermeyer, Surf. Sci. **85**, 263 (1979).
[14] A. Gerlach, G. Meister, R. Matzdorf, and A. Goldmann, Surf. Sci. **443**, 221 (1999).
[15] P. Heimann, H. Miosga, and H. Neddermeyer, Phys. Rev. Lett. **42**, 801 (1979).
[16] R. Courths, H. Wern, U. Hau, B. Cord, V. Bachelier, and S. Hüfner, J. Phys. F: Met. Phys. **14**, 1559 (1984).
[17] M. Sastry, K. C. Prince, D. Cvetko, A. Morgante, and F. Tommasini, Surf. Sci. **271**, 179 (1992).
[18] R. Koch, M. Borbonus, O. Haase, and K. Rieder, Appl. Phys. A **55**, 417 (1992).
[19] A. Nduwimana, X. G. Gong, and X. Q. Wang, Appl. Surf. Sci. **219**, 129 (2003).
[20] K. M. Ho and K. P. Bohnen, Phys. Rev. Lett. **59**, 1833 (1987).
[21] C. Hofner and J. W. Rabalais, Phys. Rev. B **58**, 9990 (1998).
[22] M. Higashiguchi, Ph.D. thesis, Hiroshima University, 2008.
[23] We have estimated the mass along the $\overline{Y\Gamma}$ direction as $m^*=(0.13\pm0.01)m_e$.
[24] G. Nicolay, F. Reinert, F. Forster, D. Ehm, S. Schmidt, B. Eltner, and S. Hüfner, Surf. Sci. **543**, 47 (2003).
[25] A. Y. Lozovoi and A. Alavi, Phys. Rev. B **68**, 245416 (2003).
[26] S. H. Liu, C. Hinnen, C. N. V. Huong, N. R. Detacconi, and K. M. Ho, J. Electroanal. Chem. Interfacial Electrochem. **176**, 325 (1984).
[27] C. H. Xu, K. M. Ho, and K. P. Bohnen, Phys. Rev. B **39**, 5599 (1989).
[28] F. Schiller, J. Cordon, D. Vyalikh, A. Rubio, and J. E. Ortega, Phys. Rev. Lett. **94**, 016103 (2005).
[29] F. Forster, A. Bendounan, J. Ziroff, and F. Reinert, Phys. Rev. B **78**, 161408(R) (2008).
[30] L. Barbier, B. Salanon, J. Sprosser, and J. Lapujoulade, Surf. Sci. **287-288**, 930 (1993).
[31] R. A. Bartynski and T. Gustafsson, Phys. Rev. B **33**, 6588 (1986).
[32] N. Memmel, Surf. Sci. Rep. **32**, 91 (1998).
[33] P. Straube, F. Pforte, T. Michalke, K. Berge, A. Gerlach, and A. Goldmann, Phys. Rev. B **61**, 14072 (2000).
[34] J. Hayoz, T. Pillo, D. Naumovic, P. Aebi, and L. Schlapbach, Surf. Sci. **433-435**, 104 (1999).